COBEM 2021 26th International Congress of Mechanical Engineering
November 22-26, 2021, Virtual Congress, Brazil

COB-2021-0362
COMPARATIVE STUDY BETWEEN GALVANIZED AND STAINLESS STEEL APPLIED IN INDUSTRIAL EQUIPMENTS UNDER DYNAMIC AND NONLINEAR BEHAVIOR

Paulo Almir Borges de Sousa Filho
José Benaque Rubert
UFSCar - Universidade Federal de São Carlos, Rodovia Washington Luís, km 235 - SP-310, São Carlos, CEP 13565-905
paulo.absfilho@gmail.com; benaque@ufscar.br

Abstract. *The current investigation is focused on the evaluation of different materials applied in steel structures builds for cooling tower equipments, in this case stainless and galvanized steel. These equipments are largely found in industries, e.g. sugarcane, and can be exposed to corrosion due to process fluid properties. This alongside with vibrations can lead to failure. It becomes necessary analyze the structural integrity verifying critical points and overall displacements, loads and stresses. The analysis is based on the stiffness method using three-dimensional truss elements, with static and dynamic modules. For the time dependent part, the Newmark's algorithm is applied considering the system unconditionally stable regardless the time step adopted. An elastic-linear work hardening constitutive model is used to describe the elasto-plastic behavior of the materials, while corrosion is considered as a homogeneous reduction in the cross-section area. Nonlinear finite element codes were written in FORTRAN and examples from the literature were analyzed to verify the accuracy of the results. For the study-case the input loads were based on data collected over field software. Both static and dynamic analysis are executed, for both non-corroded and corroded elements, stablishing a comparison between the effects of nonlinearities and structure response for the materials.*

Keywords: *computational simulation, corrosion, nonlinear dynamics, physical nonlinearity, steel structures*

1. INTRODUCTION

Understanding the nonlinear dynamic behavior of structures with respect to the type of material used in their construction is an important and necessary part of the development of industrial machinery and equipment design, including cooling towers as the one that is the main focus of the current study. These equipments are largely found in industries, such as sugarcane, under various sets that can be arranged in single or multi cells according to the requested refrigeration capacity. They are most utilized for temperature maintenance and control of processes, in applications such as wort vats, lubrication systems, among others. The drive systems are usually composed by an electric motor coupled to a speed reducer associated with a propeller. Due to process fluid properties the structural components can be exposed to corrosion. Vibrations from the drive system or from unbalanced propeller can be passed on from one modular structure to another when assembled together.

It becomes necessary analyze the structural integrity under different input conditions verifying critical points and overall displacements, loads and stresses imposed on the equipment that can lead to its collapse, as exemplified in Figure 1 (Mercury, 2013). The analysis is based on the stiffness method using three-dimensional truss elements, with static and dynamic modules. For the time dependent part, the Newmark's algorithm is applied with parameters chosen so the system is unconditionally stable regardless the time step adopted. Lumped mass matrices for space truss elements are used to describe the effects associated to mass in the dynamic analysis. Spring element models are also implemented to allow further possible changes in the structure geometry. An elasto-plastic with work hardening constitutive model is used to describe the elasto-plastic behavior of the materials. Corrosion is considered as a homogeneous reduction in the cross--section area, proportional to the original element area. For the numerical analysis, nonlinear finite element codes were written in FORTRAN language in Linux-Ubuntu environment.

Numerical simulations of known behavior structures were carried out to verify the accuracy of the results from the routines simulations. For the study-case the input loads were based on data collected over reliability and predictive maintenance field software. Both static and dynamic analysis are executed, first considering non-corroded galvanized and stainless steel elements. A comparison between the strains results are shown in order to explicit the differences between elastic and elasto-plastic behavior, also verifying if force increments contribute to differences in the obtained strains. The same procedure is repeated, this time considering uniform corrosion along elements. Considering the limitations of the proposed model, the main results are presented stablishing a comparison between the effects of nonlinearities and structure response for both materials.

Figure 1. Before and after collapse – Cooling tower structure

The analysis is conducted considering the direct stiffness approach with conditions imposed on the structures, such as: excitation model (static or dynamic); global geometry (small strains or large strains); types of constituent elements and associated degrees of freedom; material properties of elements (linear or nonlinear); types of geometric section (constant or variable), links between nodes and support reactions, as discussed by Sauoma (1999). The results achieved by the simulations, whether static or dynamic, depend on the constitutive relationship adopted to properly represent the properties. It is worth considering that the factors mentioned above impact the computational cost prior to solving the problem. The following paragraphs present some of the studies related to the research area that had an impact in the study developed in this work.

Lee et al (2017) proposes an alternative procedure for finite element analysis in structures considering the damping effect. Using a nodal approach and assuming the idealization of concentrated masses, it uses a variation of the implicit method of integration of Newmark, in order to incorporate the advantages obtained by the explicit models from an incremental procedure. The proposed method considers the damping matrix proportional to the structure, with the implementation of a model for its diagonalization. The model operates from the parameter conditions of the Newmark model for an unconditionally stable system (constant mean acceleration method) with the size of the time steps inherent to the structure stability. The accuracy and convergence is based on numerical tests of the solution against a tolerance defined from the literature. The results obtained are similar to the Newmark method, with the advantage of dealing with discontinuities and disproportionate damping without the implementation of specific strategies, turning it into a robust model for dynamic analysis of structures with damping effect.

Bai and Zhang (2013) study the nonlinear dynamic behavior of a roof metallic structure, when subjected to the condition of transient loading derived from the wind's action. It considers in the analysis the nonlinearities relevant to the geometry and constituent materials of the structures, performing simulation for a lattice and an arched type of structure. It proposes the use of limitation mechanisms in regions that are more susceptible to collapse resulting from imposed loads, either by associating a set with bilinear or self-centering behavior. Strain limiting devices replace elements that undergo significant compression and have a high level of ductility. They assume the function of "fuses" of the associated structure, with damage being concentrated on pre-selected devices and preserving the general integrity of the structure subjected to loads from wind action.

Stojanovic et al (2020) evaluates the nonlinear behavior of the vibrations of a coupled beam-arc system, evaluating the viscoelastic behavior. This physical model which is similar to the one that describes the structure of a bridge makes it possible to correlate the effect of vibration modes under different excitation conditions, verifying the influence of the coupling between the system elements and their relationship with the vibration regime. The dynamic model simulations use the Newmark method for solution and seek to demonstrate the benefits of structure stabilization via nonlinear dynamic absorption, reducing the amplitude of the effects on the excited elements.

Li et al (2018) develop a constitutive model to describe the mechanical properties of bars under the effect of corrosion. The model is based on the assumption that the corrosion effect on steel bars only impacts the reduction of the cross-sectional area. A bilinear elastoplastic constitutive equation that correlates stress-strain with the nature of pitting corrosion is validated from experimental data.

The paragraphs above seek to illustrate some of the works conduct in the study of nonlinear behavior and present some of the techniques used in the analysis. The objective of this present research is to estimate the effects of how material changes can affect the response of a steel structure of a cooling tower. For this it will be compared two types of material, galvanized structural steel S235 W covered in hot-dip zinc, which has a thicker corrosion protection layer, and stainless steel 304. In order to accomplish this objective a set of routines capable of predict the structure response for nonlinear dynamic and static behavior is developed.

2. MATHEMATICAL MODEL AND NUMERICAL SIMULATION

A finite element method procedure is applied to the structures using an approach similar to the presented in Logan (2012) by Eq. (1) through Eq. (14), that describes the structure behavior related to a mass-spring-damper system. Equation

(1) describes the overall dynamic movement of a structure, where: M=mass matrix; C=damper matrix; K=stiffness matrix; F=force vector; x=displacement vector; $\dot{x}$= velocity vector; $\ddot{x}$= acceleration vector.

$$[M]\ddot{x} + [C]\dot{x} + [K]x = [F] \tag{1}$$

The structures are described by truss or spring elements that can be modeled as shown in Figure 2 (Logan, 2012). The illustration presents an element in a 3D reference system composed by one nodal point (1, 2) in each end, with 3 degrees of freedom (DOF) each one, related to translational in x, y and z axis. The variables shown are listed as: (x', y', z') and (u', v', w'), local reference system; (x, y, z) e (u, v, w), global reference system; (u_1', v_1', w_1'), node 1 local coordinates; (u_2', v_2', w_2'), node 2 local coordinates; f'$_1$, applied force with direction along the element in node 1; f'$_2$, applied force with direction along the element in node 2; (θx, θy, θz), direction cosines related to x, y e z, respectively. The structure description as nodal points simplify the geometry calculations for each element, by informing the nodal coordinates and which nodes are associated that form an element. This also allows to further code development in order to solve n-elements systems. Equation (2) through Eq. (5) present the calculations for length (L) and direction cosines (C_x, C_y, C_z). The index coefficients (i,j) refer to each node, being the element k derived from the association of nodes i and j.

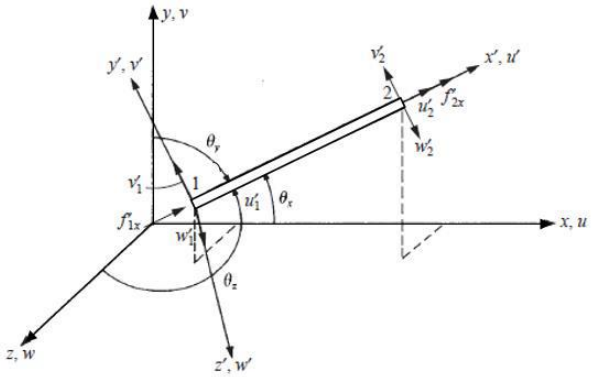

Figure 2. Truss element

$$L_k = \sqrt{\left(u'_j - u'_i\right)^2 + \left(v'_j - v'_i\right)^2 + \left(w'_j - w'_i\right)^2} \tag{2}$$

$$C_{x,k} = \frac{u'_j - u'_i}{L_k} \tag{3}$$

$$C_{y,k} = \frac{v'_j - v'_i}{L_k} \tag{4}$$

$$C_{z,k} = \frac{w'_j - w'_i}{L_k} \tag{5}$$

The stiffness matrix can be defined as Eq. (6), where T is the rotational matrix obtained by the direction cosines, k is the local stiffness matrix and K is the rotated matrix with the contribution of the element to the global stiffness matrix. The matrix form is presented in Eq. (7), where K_{st} can assume different values accordingly to which types of element and request are used.

$$K = [T]^T[k][T] \tag{6}$$

$$K = K_{st}\begin{bmatrix} C_x{}^2 & C_xC_y & C_xC_z & C_x{}^2 & C_xC_y & C_xC_z \\ & C_y{}^2 & C_yC_z & C_xC_y & C_y{}^2 & C_yC_z \\ & & C_z{}^2 & C_xC_z & C_yC_z & C_z{}^2 \\ & & & C_x{}^2 & C_xC_y & C_xC_z \\ & & & & C_y{}^2 & C_yC_z \\ Symmetry & & & & & C_z{}^2 \end{bmatrix} \tag{7}$$

$$K_{st,truss\_e} = \frac{EA}{L} \tag{8}$$

$$K_{st,truss\_p} = \frac{E_T A}{L} \tag{9}$$

$$K_{st,spring} = k_e \tag{10}$$

Equation (8) and Eq. (9) present the coefficient for a truss in elastic behavior ($K_{st,truss\_e}$)and elasto-plastic behavior ($K_{st,truss\_p}$), respectively, as can be seen by the terms E (Young's modulus) and E_T (elasticity modulus adapted for plasticity). Truss and spring elements are treated as ideals without damping effects. Since the damping effects are neglected and there are no damper elements in the structure, the damping matrices (C) assume null value. Equation (10) presents the formulation for spring elements ($K_{st,spring}$), that only depend of the spring stiffness coefficient (k_e).

The mass matrix (M_{lumped}) is formulated based on the lumped-matrix approach, that uses a diagonalization matrix as shown in Eq. (12). This allows to describe the element mass within respect to their respective nodes and also possible implementation of nodal one-off masses. For truss elements the coefficient m, presented in Eq. (11), is related to the density (ρ), area (A) and length (L) of each element, and allows to describe structures with elements of different material types. Spring elements are treated as ideals, without mass.

$$m = \frac{\rho AL}{2} \tag{11}$$

$$M_{lumped} = m\begin{bmatrix} 1 & \dots & \dots & \dots & \dots & 0 \\ 0 & 1 & 0 & 0 & 0 & \vdots \\ \vdots & 0 & 1 & 0 & 0 & \vdots \\ \vdots & 0 & 0 & \ddots & 0 & \vdots \\ \vdots & 0 & 0 & 0 & 1 & \vdots \\ 0 & \dots & \dots & \dots & \dots & 1 \end{bmatrix} \tag{12}$$

For the static analysis, invariable with time, a force vector (F) with dimensions relative to the the total number of degrees of freedom of the structure is used. For the dynamic analysis is used a matrix with dimensions that consider the DOFs and number of increments applied in the simulation. This allows for implementation of different force profiles. The static analysis can be solved through direct solution of Eq. (1) that is simplified into Eq. (13), since there is no time-dependent variable, therefore the contributions related to velocity and acceleration are null.

$$[K]\{d\} = \{F\} \tag{13}$$

The stresses (σ_k) are calculated for each element accordingly to the type of behavior, elastic or elasto-plastic. For the elastic analysis the stresses can be obtained by Eq. (14), where d corresponds to the displacement vector and is present at Eq. (15) representing the displacements associated to nodes i and j from element k.

$$\sigma_k = \frac{E_k}{L_k}\begin{bmatrix} -C_{x,k} & -C_{y,k} & -C_{z,k} & C_{x,k} & C_{y,k} & C_{z,k} \end{bmatrix}\{d\} \tag{14}$$

$$\{d\} = \begin{bmatrix} u_i & v_i & w_i & u_j & v_j & w_j \end{bmatrix}^{-1} \tag{15}$$

For the elasto-plastic simulation, a work hardening constitutive model is considered to treat the plastic side as proposed to Wierzbicki (2013) and Kim (2015). A representation is shown at Figure 3 (Wierzbicki, 2013), where after yielding (σ_y) the material behaves following a proportional constant (E_h) derived from the Young's modulus, usually 0.2E. The force increments applied to the structures characterizes a subsystem of the dynamic analysis, without the time dependent variables.

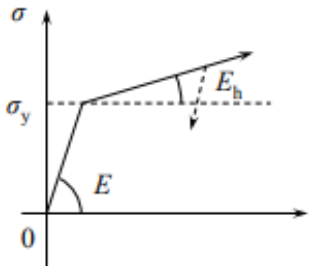

Figure 3. Stress x strain (work hardening elasto-plastic model)

By considering plasticity through work hardening modeling as presented by Kim (2015) in Eq. (16) through Eq. (18), while in the elastic domain the element response is equal as shown in Eq. (14). When enters in the plasticity domain it behaves as Eq. (16), with the effect being divided in two parts, one from elastic deformation and other from plastic deformation. An initial value for $\varepsilon_{plastic}$ can be achieved by Eq. (17), where ε_{total} is known from the calculated displacements. This initial approximation is used in Eq. (16) and the convergence criteria (δ) presented in Eq. (18) is checked, the process is iterated until the condition is satisfied. The initial approximation turns the number of iterations to be less even using a total Lagrangian approach. Figure 4 (Kim, 2015) illustrates how the procedure is conducted.

$$\sigma_k = E\varepsilon_{elastic} + E_h\varepsilon_{plastic} \tag{16}$$

$$\varepsilon_{plastic} = \frac{\varepsilon_{total}}{1+\frac{E_h}{E}} \tag{17}$$

$$|{\sigma_k}^{n+1} - {\sigma_k}^{n}| < \delta \tag{18}$$

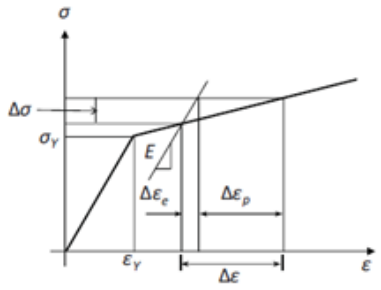

Figure 4. Stress x strain (combined elastic and plastic deformations)

In order to solve Eq. (1), the dynamic analysis is based on the Newmark method, implicit and of second order, as presented by Naeim and Anderson (2012) by Eq. (19) through Eq. (31). It consists in the time integration of Eq. (1) using defined constants β and γ. While β impacts in accelerations ($\ddot{v}$) within respect of the displacement domain, γ affects the accelerations within respect of the velocities domain. These constants are implemented in expressions that stablish a relationship between the mass, damping and stiffness matrices, being capable of describing the structure response in the time domain. The values for β and γ were defined as de γ=0.5 e β=0.25, so the system is unconditionally stable regardless the time step adopted. The equations that govern the method are present in Eq. (19) and Eq. (20) corresponding to velocity ($\dot{v}$) and displacement (v), respectively. The initial procedure follows Eq. (21) through Eq. (24) and for each time increment (Δ_t) operations are executed accordingly to Eq. (25) through Eq. (31), where: $\bar{K}$, effective stiffness matrix; A_{AUX} and B_{AUX}, auxiliary support variables; $\Delta\bar{F}$, force increments; Δv_i, $\Delta\dot{v}_i$ and $\Delta\ddot{v}_i$, additive increments related to displacement, velocity and acceleration, respectively.

$$\dot{v}(t\ +\ \Delta_t) =\ \dot{v}(t\ ) +\ (1\ -\gamma\ )\ddot{v}(t)\Delta_t +\ \gamma\ \ddot{v}(t+\Delta_t)\Delta_t \tag{19}$$

$$v(t\ +\ \Delta_t) =\ v(t\ ) +\ \dot{v}(t)\Delta_t + \left(\frac{1}{2} - \beta\right)\ddot{v}(t){\Delta_t}^2 + \beta\ddot{v}(t\ +\ \Delta_t){\Delta_t}^2 \tag{20}$$

$$\ddot{v} = \frac{F(0) - C\dot{v}(0) - Kv(0)}{M} \tag{21}$$

$$\bar{K} = K + \frac{\gamma}{\beta\Delta_t}C + \frac{1}{\beta(\Delta_t)^2}M \tag{22}$$

$$A_{AUX} = \frac{1}{\beta\Delta_t}M + \frac{\gamma}{\beta}C \tag{23}$$

$$B_{AUX} = \frac{1}{2\beta}M + \Delta_t\left(\frac{\gamma}{2\beta} - 1\right)C \tag{24}$$

$$\Delta\bar{F} = \Delta\bar{F} + A_{AUX}\dot{v}_i + B_{AUX}\ddot{v}_i \tag{25}$$

$$\Delta v_i = \frac{\Delta\bar{F}}{\bar{K}} \tag{26}$$

$$\Delta\dot{v}_i = \frac{\gamma}{\beta\Delta_t}\Delta v_i - \frac{\gamma}{\beta}\dot{v}_i + \Delta_t\left(1 - \frac{\gamma}{2\beta}\right)\ddot{v}_i \tag{27}$$

$$\Delta\ddot{v}_i = \frac{1}{\beta(\Delta_t)^2}\Delta v_i - \frac{1}{\beta\Delta_t}\dot{v}_i - \frac{1}{2\beta}\ddot{v}_i \tag{28}$$

$$v_{i+1} = v_i + \Delta v_i \tag{29}$$

$$\dot{v}_{i+1} = \dot{v}_i + \Delta\dot{v}_i \tag{30}$$

$$\ddot{v}_{i+1} = \ddot{v}_i + \Delta\ddot{v}_i \tag{31}$$

The algorithm for the static nonlinear solution can be found in Table 1. Table 2 presents the simplified steps for the algorithm that generates the force profile that is applied to nodes in the dynamic analysis. Table 4 shows the logical algorithm behind the dynamic analysis, with Table 3 expanding the particularities for implementation of the Newmark method.

Table 1. Simplified steps for algorithm implementation – Static nonlinear analysis

Variables declaration and sizing
Opening and reading of input parameters
do i=1,number of elements
Elements generation
Calculation of geometrical properties and cosines direction
Assembly of local stiffness matrices
Coefficient attribution in global stiffness matrix
do i=1,number of solution nodes
Solution matrix generation
do i=1,number of total degrees of freedom
Calculation of displacements
Calculation of stresses
if (stress> yielding point)
Decomposition between elastic and plastic strains
Iteration until convergence criteria is achieved
Calculation of strain
elseif (stress ≤ yielding point)
Elastic response
Calculation of resulting forces

Table 2. Simplified steps for force profile generation – dynamic nonlinear analysis

Variables declaration and sizing
Opening and reading of input parameters
Calculation of time dependent variables
do i=1,number of solution nodes
do=1, number of time steps
Calculation of forces applied in nodal points accordingly with govern equation
do i=1,number of total degrees of freedom
do=1, number of time steps
Coefficient attribution in force matrix
Matrix export to registry file

Table 3. Simplified steps for Newmark method implementation – dynamic nonlinear analysis

do i=1,number of solution nodes
Declaration of Newmark and boundary conditions parameters $(v(0) = 0, \dot{v}(0) = 0)$
Initial calculation of acceleration $\ddot{v}(0)$
Calculation of effective stiffness matrix $\bar{K}$
Calculation of auxiliar parameter A_{AUX}, B_{AUX}
do=1, number of time steps
do i=1,number of solution nodes
Calculation of forces increments $\Delta\bar{F}$
Calculation of displacement increments Δv_i
Calculation of velocities increments $\Delta\dot{v}_i$
Calculation of acceleration increments $\Delta\ddot{v}_i$
Calculation of variable for next time step $v_{i+1}, \dot{v}_{i+1}, \ddot{v}_{i+1}$

Table 4. Simplified steps for algorithm implementation – dynamic nonlinear analysis

```
Variables declaration and sizing
Opening and reading of input parameters
    do i=1,number of elements
        Elements generation
        Identification of type of element (damper/ spring/ truss)
        Calculation of geometrical properties and cosines direction
        Assembly of local stiffness matrices
        Multipliers for spring elements
        Coefficient attribution in global stiffness matrix
    do i=1,number of solution nodes
        Solution stiffness matrix generation
    do i=1,number of elements
        Assembly of local mass matrices
        Multipliers for mass elements
        Coefficient attribution in global mass matrix
        Attribution of one-off nodal masses in global mass matrix
    do i=1,number of solution nodes
        Solution mass matrix generation
        Attribution of one-off nodal masses in global mass matrix
    do i=1,number of total degrees of freedom
        do=1, number of time steps
            Reading of force profile registry
    do i=1,number of solution nodes
        do=1, number of time steps
            Declaration of Newmark and boundary conditions parameters
            Initial calculation for Newmark method
            Application of Newmark method
            Calculation of displacement, velocity and acceleration
    do i=1,number of total degrees of freedom
        do=1, number of time steps
            Stresses calculation
            Resulting structure forces calculation
```

The study case made use of the materials with properties as presented in Table 5. Figure 5 shows the geometrical configuration, main dimensions and linked nodes of the structure. The structure contains 16 nodes with boundary conditions that restrain movement in x, y and z axis of node 3, restrain in axis y and z of node 4, restrain in axis x and z of node 2 and restrain in axis z of node 1, resulting in 40 degrees of freedom with no restriction in movement. The elements are made by the association of two nodes (i,j) and initial areas identified in Figure 5. Forces (F) that increase linearly with time are applied to the nodes 13 and 16 of the structure by a period of 30 seconds, resulting in a total of 30kN. After that no force is applied. The total simulation time corresponds to 40 seconds with time increments of 0.5 seconds. The mass of the driven system of 1,543.6kg on top of the structure is treated as one-off masses in nodes 13, 14, 15 and 16 with one quarter of the total system mass in each node. The structure is described by elements from the same material but a mixed composition is also possible to simulate if desired.

Metal structures with application in cooling towers are commonly built from the materials presented. Although stainless steel has superior corrosion and abrasive wear resistance compared to structural S235 W, both are considered under the same conditions in the simulations. This is to verify only the behavior of alloys in terms of requests, evaluating stresses, deformations in the elements and geometrical changes in the structure. Steel S235 W uses a hot-dip zinc coating layer with a thickness of 2.35oz/ft², equivalent to 305.152g/m², while stainless steel is obtained from the insertion of a percentage of chromium in the alloy. Commercially, 304 stainless steel is about three times the cost of S235 W structural steel. The comparison of the structure's behavior regarding its stiffness and the verification of the possible occurrence of failures in elements is carried out to identify the elements most affected by the requests and to determine positions for the use of premium materials.

Table 5. Material properties for galvanized structural steel S235 W and stainless steel 304

	Density [Mg/m³]	Elastic Limit [MPa]	Tensile Strength [Mpa]	Poisson's Ratio	Shear Modulus [GPa]	Young's Modulus [GPa]
Structural Steel with galvanized coating S 235W (EN-10025-5)	7.85	215	360	0.3	81	210
Stainless steel Grade 304 (UNS S30400)	7.955	250	565	0.27	78	196

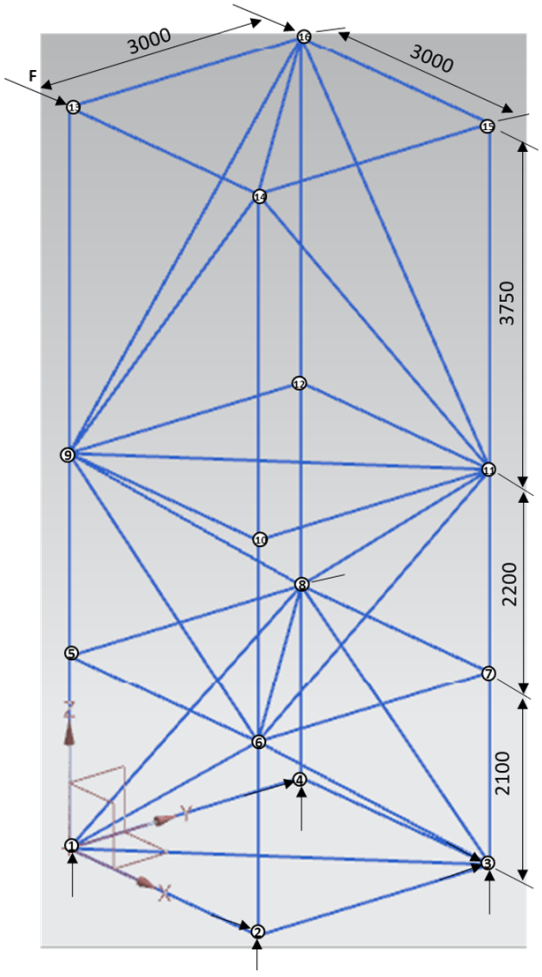

Element k	node i	node j	Area [cm²]
Element 1	1	4	48,10
Element 2	1	2	48,10
Element 3	2	3	48,10
Element 4	3	4	48,10
Element 5	1	3	7,67
Element 6	1	8	7,67
Element 7	1	5	79,10
Element 8	1	6	7,67
Element 9	2	6	79,10
Element 10	3	6	7,67
Element 11	3	7	79,10
Element 12	3	8	7,67
Element 13	4	8	79,10
Element 14	5	8	48,10
Element 15	5	6	48,10
Element 16	6	7	48,10
Element 17	7	8	48,10
Element 18	6	8	7,67
Element 19	5	9	79,10
Element 20	6	9	7,67
Element 21	6	10	79,10
Element 22	6	11	7,67
Element 23	7	11	79,10
Element 24	8	11	7,67
Element 25	8	12	79,10
Element 26	8	9	7,67
Element 27	9	12	48,10
Element 28	9	10	48,10
Element 29	10	11	48,10
Element 30	11	12	48,10
Element 31	9	11	7,67
Element 32	9	16	7,67
Element 33	9	13	79,10
Element 34	9	14	7,67
Element 35	10	14	79,10
Element 36	11	14	7,67
Element 37	11	15	79,10
Element 38	11	16	7,67
Element 39	12	16	79,10
Element 40	13	16	92,40
Element 41	13	14	92,40
Element 42	14	15	92,40
Element 43	15	16	92,40
Element 44	14	16	7,67

Figure 5. Structure composition and geometrical properties

3. RESULTS

The simulations considered the situations as listed, being without corrosion and with 50% of homogeneous corrosion in elements with cross sectional area of 48,1cm² and 7,67cm². As explained earlier the corrosion was treated as a decrease in the cross-sectional area of each element. In order to verify differences of behavior in the structure graphs of displacement, velocities and accelerations were generated, as present in Figure 6 with time dependent curves for each degree of freedom of the structure without corrosion of stainless-steel grade 304. Graphs in Figure 6 are similar for the structure under the effect of corrosion, but with greater amplitude. Elements were selected based on the stress level in order to show the differences in behavior when considering response in plastic regime. Thus, stress x strain graphs were generated for each pre-selected element (34 and 36), as shown in Figure 7, for both cases, without corrosion and with corrosion in the structure, respectively. The analysis was repeated for galvanized structural steel, with the results being presented in Figure 8. Table 6 brings together the main differences found between the results.

Table 6. Results for strain and stress in elements 34 and 36

	Stainless steel 304 (UNS S30400)			**Structural steel with galvanized coating S 235W (EN-10025-5)**		
	Non corroded	50% corroded	50% corroded (elastic)	Non corroded	50% corroded	50% corroded (elastic)
Strain element 34	6,390E-04	7,680E-03	2,505E-03	4,610E-04	4,890E-03	1,667E-03
Stress element 34 [Pa]	1,250E+08	5,010E+08	5,010E+08	8,760E+07	3,500E+08	3,500E+08
Strain element 36	3,200E-04	2,340E-03	1,460E-03	3,300E-04	2,280E-03	1,320E-03
Stress element 36 [Pa]	6,270E+07	2,920E+08	2,920E+08	6,270E+07	2,510E+08	2,510E+08

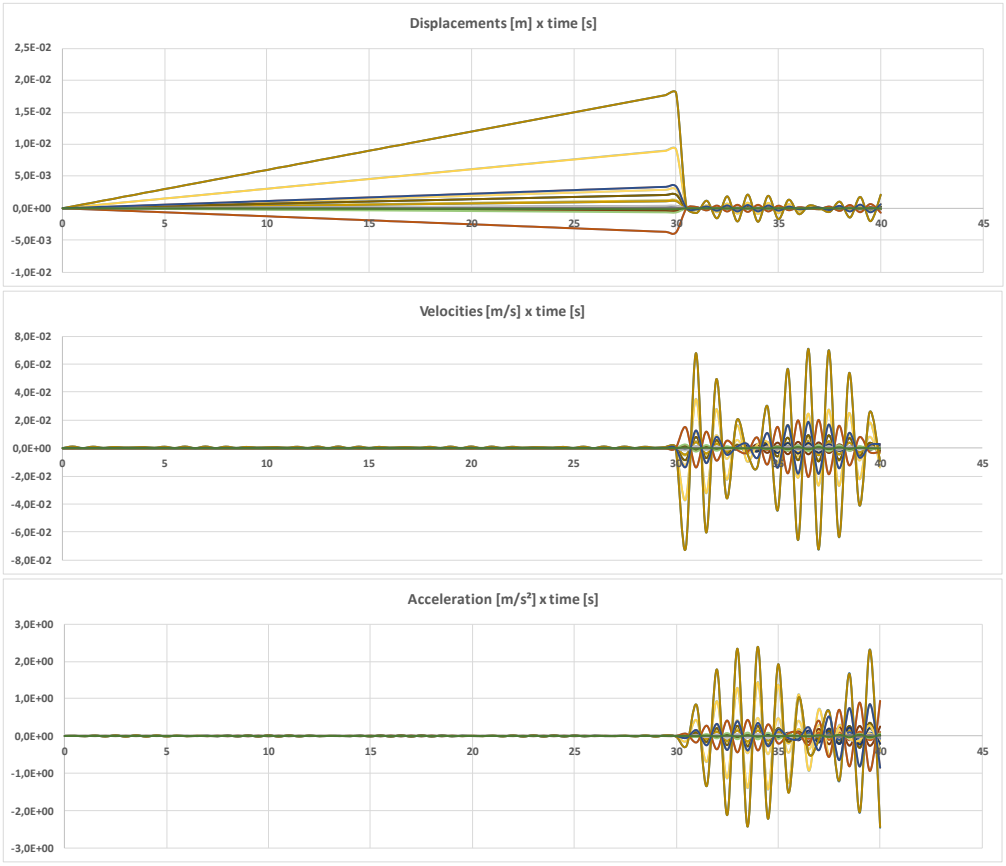

Figure 6. Dynamic behavior of structure – Stainless steel grade 304

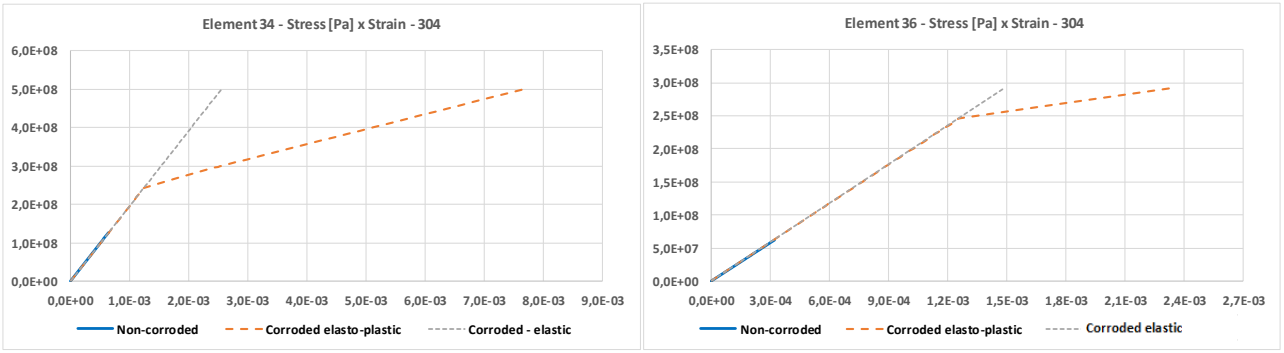

Figure 7. Stress x Strain curves for non-corroded and corroded elements – Stainless steel grade 304

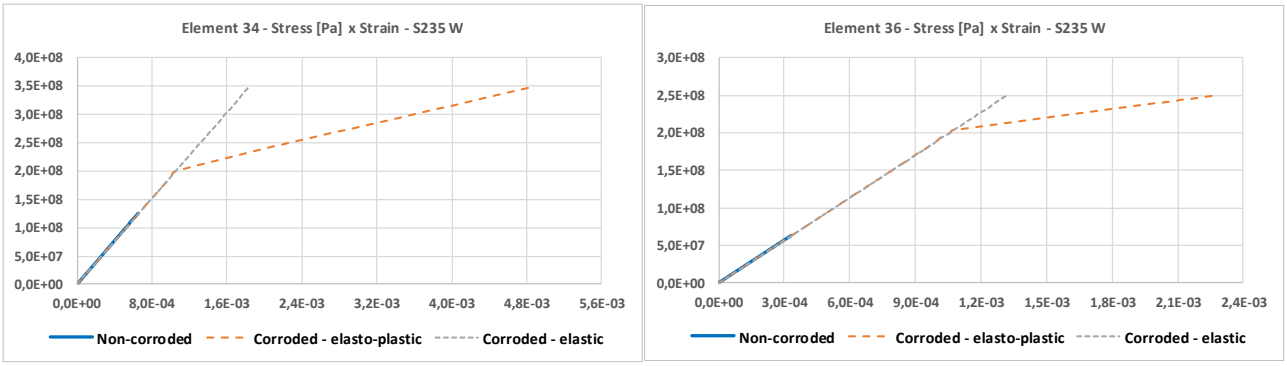

Figure 8. Stress x Strain curves for non-corroded and corroded elements – Galvanized structural steel S235 W

4. CONCLUSIONS

It is noted in Figure 6 that both velocity and acceleration admit values close to zero during the loading phase, given the load increments imposed on the structure. After the abrupt removal of forces (F) from the structure, it is observed that the geometric arrangement seeks to reach equilibrium again, with a response in the field of velocities and accelerations. It is also verified that the time of 10s without applying forces to the structure is not enough for its stabilization. The use of spring-damper elements at strategic points could help to attenuate the response and reduce the time for stabilization. For example, considering that larger displacements occur in GDL 46, the implementation of a spring-damper element in the x-axis direction at node 16 could reduce the structure response attenuation time.

It is observed that the curves “Corroded elasto-plastic” and “Corroded elastic” presented in Figure 7 and Figure 8 contrast the type of analysis performed on the structure. If only the elastic response is considered, this can lead to a wrong prediction, with stresses and strains that do not effectively portray the behavior of the elements. For galvanized structural steel, it is still possible to observe that the tensile strength limit is reached, with element 34 presenting rupture and behavior in a plastic regime prior to failure. The three elements that present greater tensile stress correspond to 34, 36 and 32, in descending order. For compression, these are elements 44, 20 and 31, in descending order in module.

Comparing the structure constituted by structural steel S235 W and stainless steel 304, without the presence of corrosion, the input forces produced a maximum displacement close to 18mm. The responses for elements 34 and 36 of the structure without corrosion effect are in the elastic regime, with maximum values shown in Table 6. It is noted that the deformation associated with the same stress level for the structure without corrosion effect is about 3% lower for element 36 made of stainless steel 304, which despite having a Young's modulus of smaller magnitude, admits an upper elastic limit. For the structure with a 50% corrosion effect the elements can behave in an elastic and plastic regime, and the deformation in element 34 is about 57% higher for stainless steel 304, while in element 36 about 3% higher for stainless steel 304. This can be explained since the deformations incurred for structural steel S235 W led to material rupture. In addition to that, above the yield stress of 215 MPa, S235 W presents greater sensitivity when compared to 304 stainless steel. The values presented in the columns named “50% corrosion (elastic)” is just a simulation to present the possible misunderstanding in the prediction of behavior in the case where the plastic regime is neglected, resulting in deformations with values up to 67% lower. The work so far provides an effective set of routines, capable of predicting the behavior in elastic and plastic regimes for truss structures in the fields of dynamics and statics. Future development can be done to allow other types of elements to be simulated with code.

5. REFERENCES

Bai L., Zhang Y., 2013. *Nonlinear dynamic behavior of steel framed roof structure with self-centering members under extreme transient wind load*. Engineering Structures, v.49, pp. 819-830.

Kim, N., 2015. *Introduction to nonlinear finite element analysis*. Springer.

Lee T., Chung K., Chang H., 2017. *A new implicit dynamic finite element analysis procedure with damping included*. Engineering Structures, v.147, pp. 530-544.

Li D., Cheng X., Huang T., Wei R., Han N., Xing F., 2018. *A simplified constitutive model for corroded steel bars*. Construction and Building Materials, v.186, pp. 11-19.

Logan D., 2012. *A first course in the finite element method*. University of Wisconsin-Platteville, 5ª ed.

Mercury L., 2013. *Power station collapse*. https://www.lithgowmercury.com.au/story/1268492/power-station-collapse/. Accessed 20 June 2021.

Naeim C., Anderson C. A., 2012. *Basic structural dynamics*. John Wiley & Sons.

Saouma V. E., 1999. *Matrix structural analysis with an introduction to finite elements*. CEAE - University of Colorado.

Stojanovic V., Petkovic M. D., Milic D., 2020. *Nonlinear vibrations of a coupled beam-arch bridge system*. Journal of Sound and Vibration, v.464.

Wierzbicki T., 2013. *Lecture 12: Fundamental concepts in structural plasticity*. Structural Mechanics, MIT OpenCourseWare, https://ocw.mit.edu/courses/mechanical-engineering/2-080j-structural-mechanics-fall-2013/course-notes/mit2_080jf13_lecture12.pdf. Accessed 20 June 2021.

6. RESPONSIBILITY NOTICE

The author(s) is (are) the only responsible for the printed material included in this paper.